Study of the Dynamics of the Intertropical Convergence Zone with a Symmetric Version of the GLAS Climate Model

B. N. GOSWAMI,[1] J. SHUKLA, E. K. SCHNEIDER[2] AND Y. C. SUD

Laboratory for Atmospheric Sciences, NASA/Goddard Space Flight Center, Greenbelt, MD 20771

(Manuscript received 13 December 1982, in final form 25 August 1983)

ABSTRACT

The results of some calculations with a zonally symmetric version of the Goddard Laboratory of Atmospheric Sciences (GLAS) climate model are described. The model was first used to study the nature of symmetric circulation in response to various zonally-averaged latent heating fields based on observations. Three experiments with distribution of latent heating corresponding to the equinox condition, Northern Hemisphere summer condition and south Asian monsoon condition showed reasonable similarity to the observed distribution of surface easterlies and westerlies and the subtropical westerly jets. In the south Asian monsoon experiment, surface westerlies as well as the upper-level easterly jet in the subtropics of the Northern Hemisphere were found. The strength of the subtropical westerly jet increased with decrease in the vertical eddy viscosity.

Additional experiments were carried out in which the model was allowed to determine its own latent heat sources and the results were analyzed to examine the interaction of CISK and the imposed SST in determining the position, structure and transient behavior of the ITCZ. In the small number of cases considered, the model equilibrium was found to be independent of initial conditions, with a narrow ITCZ occurring over the SST maximum. After the equilibrium solution was established, the specified SST distribution was altered. It was found that the initial ITCZ persisted for a long time (weeks to months); however, finally a new ITCZ became established at the location of the new SST maximum. Initially its development was slow, but was followed by a rapid intensification toward the end. The time needed for the establishment of the ITCZ at its new position depended upon the latitude of maximum SST and the magnitude of the SST anomaly.

The calculations also indicated the properties of some of the parameterizations employed in the climate model, in particular, the moist convection and the effects of clouds on radiative cooling.

1. Introduction

The study of the symmetric (zonally independent) circulation has played an important role in our understanding of the general circulation of the atmosphere. In the past few decades, the symmetric circulation has been studied by many authors (e.g., Charney, 1969; Hunt, 1973; Schneider and Lindzen, 1977; Schneider, 1977; Held and Hou, 1980; Charney *et al.*[3]). The motivation for such studies, besides being a purely geophysical fluid dynamical study relevant to the symmetric circulations in rotating planets, has stemmed from the observation that the mean meridional circulation accounts for most of the poleward transports of heat and momentum in the tropics. This does not mean that the tropical circulation is symmetric. Geographical distributions of continents and oceans in the tropics result in asymmetric heat sources and sinks which are important for maintaining many of the gross features of the tropical circulation; however, some features of the tropical circulation may be examined in the context of a symmetric model. One important feature of the tropical circulation is the so-called Intertropical Convergence Zone (ITCZ), which, over the ocean, produces long tropical cloud bands in satellite pictures (Miller and Feddes, 1971). These cloud bands are not continuous around the globe at any particular instant of time. However, long-time averages of the cloudiness in the tropics show these bands to be sufficiently "symmetric" to justify their study with symmetric models. Some of the noteworthy features of the observed ITCZ can be summarized as follows (Gruber, 1972; Sadler, 1975; Estoque and Douglas, 1978, Kornfield *et al.*, 1967; Hubert *et al.*, 1969; Riehl, 1979):

1) The ITCZ seems to avoid the equator over the oceans.

2) The seasonal shift in the latitudinal position of the ITCZ is less over the oceans than over the continents—about 10–15° over the oceans and about 20–25° over the continents.

[1] Present affiliation: Center for Atmospheric and Fluid Sciences, Indian Institute of Technology, Hauz Khas, New Delhi, India.

[2] Present affiliation: Division of Applied Sciences, Harvard University, Cambridge, MA 02139.

[3] Charney, J. G., E. Kalnay, E. K. Schneider and J. Shukla, 1977: Unpublished manuscript. A study of the dynamics of the ITCZ in a symmetric atmosphere-ocean model. Paper presented at the Joint IUTAM/IUGG Symposium on Monsoon Dynamics, New Delhi, 5–9 December 1977.

3) In the North Pacific the ITCZ is located between the equator and 15°N with its maximum northward position in September–October. In the Atlantic, the ITCZ lies between the equator and 10°N with maximum northward position again during September–October. Although there is a persistent cloud band in the South Pacific extending from the tropics (Indonesian region) to the Southern Hemisphere subtropics (about 35°S), this feature is not usually referred to as an ITCZ. In the Indian Ocean the ITCZ occurs between 10°N and 10°S. There may be an occasional presence of two ITCZs on either side of the equator (Kornfield *et al.*, 1967). However, this does not appear to be a persistent phenomenon and cannot be considered as a climatological feature (Hubert *et al.*, 1969).

4) The ITCZ over land, in general, seems to follow the seasonal march of the sun. Over western Africa, it is at ~5°N during January–February and at about 22°N during August–September (see the GARP Publication Series No. 21, The West African Monsoon Experiment, 1978). Over India, during the peak monsoon season, the ITCZ is at about 25°N near the foothills of the Himalayas. This great northward extension of the ITCZ seems to be aided by the elevated heat source of the Tibetan Plateau.

5) By comparing the climatological distribution of the sea surface temperature (SST) during the months of February and August with the climatological positions of the ITCZ over the tropical oceans during the same months, Saha (1971) suggested that the oceanic ITCZ generally occurs over the regions of warm SST.

There are only a few theoretical studies of the climatological features of the ITCZ. Charney (1969) suggested that over the ocean, an ITCZ at the equator is unstable to lateral displacements. If, for instance, it is moved slightly away from the equator to the north, the induced surface easterlies will result in upwelling lowering the SST over the equator. This will prevent the ITCZ from moving back to the equator. Moreover, cyclonic shear will be generated across the ITCZ and this will enhance the frictional convergence at it. This will help maintain the ITCZ away from the equator. In a later study Charney *et al.* (1977) verified this hypothesis with a coupled ocean–atmosphere model. Pike (1971) used a simple atmosphere–ocean coupled model to study the ITCZ. His atmospheric model was zonally symmetric with β-plane geometry between 34°S and 34°N. It had ten levels in the vertical with staggered vertical resolution. The ocean model consisted of an upper mixed layer of variable height driven by the atmospheric wind stresses and a lower inert layer of fixed depth. The model had 2° horizontal resolution. He started with an almost uniform SST in the tropics between 14°S and 14°N. In the early stages of evolution of the circulation, the ITCZ appeared over the equator. However, the motion associated with the ITCZ produced upwelling which made the SST cooler at the equator and the ITCZ was subsequently found to move away from the equator to a region of SST maximum. He also found that, although the SST had two maxima, one on either side of the equator, a stable ITCZ developed on only one side of it.

For the present study, a zonally symmetric version of the Goddard Laboratory for Atmospheric Sciences (GLAS) climate model was constructed. The model contains the same physical parameterization, resolution and numerical techniques as the full climate model. The zonally symmetric version of the GCM is useful for two purposes. First, the behavior of such a model is easier to understand and explain than the behavior of the full climate model. Much of the internal variability of the GCM is due to wave activity that is not present in the zonally symmetric model. The forcing of the general circulation of the zonally symmetric model is directly and entirely due to the parameterized physical processes consisting of radiation, moist convection, and PBL fluxes from the surface. The zonally symmetric model can be used to evaluate the behavior of the parameterizations and possibly it can help in improving them. Second, the model can be used as an experimental tool. Much theoretical and numerical research has been concerned with the zonally symmetric or zonally averaged equation of motion. These studies have employed assumption and various degrees of approximations to the equation of motion which are unnecessary using the zonally symmetric GCM approach. The model can therefore be used to examine the appropriateness of these assumptions and approximations, to answer outstanding questions and to suggest new problems. One use which the model will eventually have is the representation of the atmospheric part of a dynamical model of a complete interactive zonally symmetric and internally consistent climate model, including zonally symmetric oceans and continents, as well as possibly glacial accumulation and flow, oceanic ice formation, albedo–precipitation feedbacks, and so on. Such a model could be enlightening as to the causes of climatic change.

The present article is concerned with a description of the model, its response to specified latent heat sources, and its response to the sea surface temperature as the lower boundary condition. Some modification to the GCM physics was made in these calculations, in that model-generated clouds do not interact with radiation, nor has climatological cloudiness been assumed for the radiative calculation. The cloud–radiative feedback parameterization, was found to lead to a very large amount of internal variability (which may or may not be realistic), and made interpretation of the results difficult. The response to various specified latent heat sources constructed by using climatology was considered first. Also, the models' response was examined using different internal viscosities. The present model behaves qualitatively as predicted by simple

theories (Dickinson, 1971a, 1971b: Schneider, 1977, 1983).

Next, the model was allowed to determine its own moisture and latent heating distribution. The specific feature of interest was the position and structure of the ITCZ, defined to be the latitude band of maximum precipitation, which coincides of course with the latitude band in which the strongest rising motion occurs. As the model satisfies the moisture budget, the ITCZ is the locus of maximum moisture convergence, which occurs primarily in the boundary layer due to the properties of water vapor. Because of the structure of the model, the position that the ITCZ chooses can be due either to the imposed SST distribution or to the initial condition of the integration.

Water vapor in the tropical boundary layer is enhanced by evaporation and air mass convergence. Boundary layer mass convergence in quasi-equilibrium is induced by viscous flow down the pressure gradient. Boundary layer pressure gradients are closely related to meridional temperature gradients both in and above the boundary layer. These pressure gradients can be produced by sensible and radiative heat transfer from the surface and by the release of latent heat above the boundary layer. The latent heating can be intensified by the induced boundary layer moisture convergence, and this process is called CISK. The role of CISK in the formation of the ITCZ was suggested by Charney (1971), where he used local Ekman layer theory to represent the boundary layer. This approximation is likely to be invalid near the equator (Schneider and Lindzen, 1976).

If the SST distribution is fixed, the SST induced boundary layer moisture convergence is also essentially fixed, and the maximum will occur near the latitude of maximum SST. CISK, on the other hand can operate anywhere (so long as the boundary layer moisture content is sufficient) and can be self-maintaining. CISK is also mathematically nonlinear because latent heating is only associated with upward motion. According to Charney's (1971) calculations, the most rapidly growing CISK induced ITCZ would have the narrowest possible meridional scale and would not occur at the equator. Avoidance of the equator is due to the probably incorrect representation of the equatorial boundary layer.

The mathematical nonlinearity of the CISK process allows the possibility that an equilibrium zonally symmetric ITCZ could be self-maintaining at different latitudes for the same SST distribution, with position depending on the initial conditions. Charney (1968) found this to be the case using a two-level model.

We have performed a few experiments, which are described below, in an attempt to obtain these multiple equilibria, in which the results are not in agreement with Charney's. CISK apparently is important in the model, in that the ITCZ always chooses the narrowest possible meridional scale, but the equilibrium ITCZ always eventually forms over the SST maximum. It is possible, however, to produce highly persistent ITCZ structures away from the SST maximum by a suitable choice of initial conditions so that CISK and SST effects are at least competitive.

The model is described in Section 2. The specified latent heating experiments are discussed in Section 3a. The ITCZ experiments are the subject of Section 3b. The results are summarized and discussed in Section 4.

2. Description of the model

The zonally symmetric model used in this study is obtained by setting all the longitudinal derivatives to zero in the GLAS climate model described by Shukla *et al.* (1981). Thus the symmetric model has 46 grid points (4 degree latitude grid) in the horizontal and 9 levels in the vertical. The upper boundary of the model is at 10 mb. The prognostic atmospheric variables are surface pressure, zonal and meridional components of the horizontal wind, temperature and water vapor mixing ratio.

For horizontal finite differencing the model variables are staggered according to the one-dimensional version of B-grid schemes of Arakawa and Lamb (1977). In the vertical the variables are staggered according to the scheme of Lorenz (1967). For time integration, the Matsuno forward–backward time differencing scheme is used. This scheme tends to damp the high frequency oscillation and thus helps to control computational noise.

The symmetric model uses the same parameterizations for the physical processes as used in the GLAS Climate Model. For completeness we shall briefly describe them here. The model uses cumulus parameterization developed by Arakawa (1972) for the three level UCLA GCM but as modified for use in a nine-level GCM by Sommerville *et al.* (1974). The model also includes latent heat release due to large-scale condensation. This is assumed to occur when the relative humidity exceeds 100%.

The shortwave radiation calculation follows the method developed by Lacis and Hansen (1974). It includes absorption by ozone, water vapor, carbon dioxide and clouds. The longwave parameterization is based on the method of Wu (1980). The parameterization includes a water vapor transmittance that uses a statistical band model with the strong line version of Curtis–Godson (Godson, 1955) approximation. It also includes water vapor dimer effect in the 8–13 μm window region, line-by-line precalculation of CO_2 transmittance including fundamental bands, hot bands and isotopes, tables of ozone transmittance and the effect of clouds. In order to calculate the incoming longwave flux at the top of the model (10 mb), zonally averaged climatological temperatures at 1 mb and 5 mb are prescribed.

Clouds occur if the model predicts cumulus convection (restricted to the lowest six layers) or large-scale condensation (in any layer). No parameterization of subgrid-scale fractional cloudiness is included. Both supersaturation and convective clouds are assumed to fill a grid box. In these calculations all clouds are assumed to be black bodies.

A "dry convective adjustment" is used in the model to prevent the atmosphere from being dry adiabatically unstable (i.e., $\theta_{l-1} \leq \theta_l$). If the lapse rate is unstable, the potential temperature of the upper layer (θ_{l-1}) and that of the lower layer (θ_l) are set equal to a mass weighted average potential temperature. The temperatures are then accordingly recalculated.

The planetary boundary layer parameterization in the model is a revised version (Sud and Abeles, 1981) of the parameterization used by Sommerville *et al.* (1974). A brief description of this parameterization may be found in Sud and Fennessy (1982). The revised version produces more realistic surface fluxes of evaporation and sensible heat.

The effect of momentum mixing due to "cumulus clouds" is not included in the model. The vertical eddy viscosity and diffusivity coefficient at level 5 (505 mb in our model) has been increased from approximately 0.1 $m^2 s^{-1}$ used in the GLAS Climate Model to 33 $m^2 s^{-1}$ in the symmetric model. This eddy viscosity coefficient decreases linearly with pressure in the vertical. Such a high viscosity ensures attainment of a steady state solution by the model. No horizontal diffusion is included in the model.

A 10-min time step is used to integrate the dynamics. Except for the calculation of longwave radiation, all the physical quantities are calculated every half hour. The longwave radiation calculations are performed every 4 h.

An all-ocean lower boundary is assumed for all of the experiments described in this study. Albedo for the ocean surface is taken to be 0.07. The SST prescribed for the spring simulation (permanent equinox) as well as for the summer simulation (permanent solstice) are shown in Fig. 1. These zonally averaged SSTs were obtained from mean monthly (April and August, respectively) observed sea surface temperature provided by GFDL and adopted for the symmetric GLAS Climate Model by zonally averaging and applying subjective smoothing. The initial conditions consisted of a resting atmosphere and temperature and mixing ratio, shown in Fig. 2.

After examining some of the runs of the symmetric Model we found that the Model did not yield a steady state solution. The transient activity was so large that instantaneous snapshots of the meridional circulation bore little resemblance to the (well behaved) time mean meridional circulation. The instantaneous meridional circulation appeared to have no organized large-scale structure, and there was no apparent correlation between the meridional circulation at adjacent time steps.

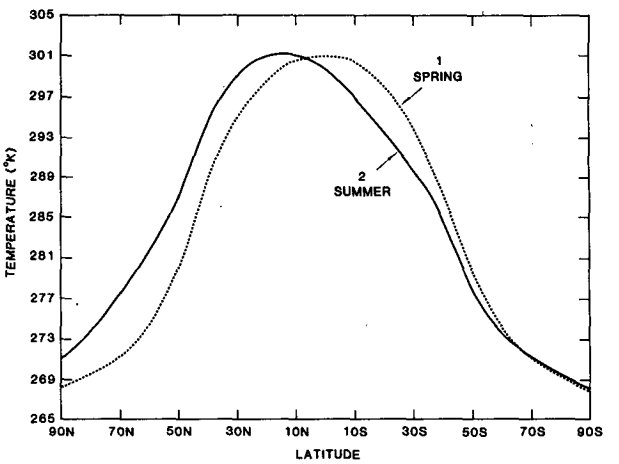

FIG. 1. Sea surface temperature prescribed for various experiments. Curve 1 corresponds to equinox condition and curve 2 corresponds to Northern Hemisphere summer condition.

This transient activity was not suppressed, even by large internal viscosity. The primary reason for this variability was found to be the interactive cloud–radiative feedback calculation in the model. The mechanism by which the interactive cloud–radiative feedback produces transients is under investigation. It is quite possible that the model representation of the effects of cloud–radiative feedback are unrealistic, and that a better parameterization would not produce such large internal variability. For the purposes of obtaining more easily interpretable results, cloud-radiative feedback was suppressed by ignoring all clouds as far as the radiative calculations are concerned. This modification has the somewhat undesirable effect of increasing the outgoing longwave radiation (i.e. increasing the apparent solar constant) when SSTs are specified, as thermal emission escapes to space from a lower and therefore warmer atmospheric level. The experiments described in this paper are summarized in Table 1.

3. Experiments

a. Fixed heat source experiments

In order to better understand the properties of the moist convection parameterization, the effect of neglecting the influence of clouds in the radiative calculations, and as a partial verification of the model, some experiments with prescribed time-invariant latent heat sources were carried out. However, a climatological water vapor distribution was used for the radiative calculations.

There are a few somewhat more idealized model calculations which predict the expected qualitative behavior of the equilibrium solutions to these latent heating experiments. Dickinson (1971a,b) examined the equilibrium response of a linearized, equatorial β-plane model to idealized ITCZ latent heating both at

TABLE 1. A brief description of various experiments discussed in this study. For all runs, the radiative heating and sensible heat flux are calculated using parameterizations of the GLAS Climate Model.

Experiment	Referred in the text as	SST used	Position of the sun fixed at	Vertical eddy viscosity coefficient at level 5 ($m^2 s^{-1}$)	Latent heating
1	ITCZ/Symmetric Circulation: Equinox	Curve 1 of Fig. 1	Equator	33	Prescribed (Q_1) from Newell *et al.* (1974) March–April–May average. Fig. (5a)
2	ITCZ/Symmetric Circulation: Northern Hemisphere Summer	Curve 2 of Fig. 1	15°N	33	Prescribed (Q_2) similar to JJA average of Newell *et al.* (1974). Fig. (6a)
3	ITCZ/Symmetric Circulation: Monsoon	Curve 2 of Fig. 1	15°N	33	Prescribed and constructed by us.
4	Response to broad tropical heat source: Equinox	Curve 1 of Fig. 1	Equator	16.5	Modified Q_1. Same precipitation distribution as Q_1. Horizontal and vertical distribution modified between 15°S–15°N.
5	ITCZ with no latent heating	Curve 2 of Fig.1	15°N	33	None
6	Role of vertical eddy viscosity: Equinox	Curve 1 of Fig. 1	Equator	33 16.5 6.6	Same as Q_1
7	Role of vertical eddy viscosity: Equinox	Curve 1 of Fig. 1	Equator	33 16.5 6.6	Same as Q_1
8	ITCZ/Ocean run: Equinox	Curve 1 of Fig. 1	Equator	33	Calculated by the model physics
9	ITCZ/Ocean run: Northern Hemisphere Summer	Curve 2 of Fig. 1	23.5°N	33	Calculated by the model physics
10	Response of ITCZ to displacement of SST from 14°N to 2°N	Curve 1 of Fig. 1	15°N	33	Calculated by the model physics
11	Response of ITCZ to displacement of SST from 14°N to 2°N	Curve 2 of Fig. 1, with maximum at 2°N	15°N	33	Calculated by the model physics
12	Response of ITCZ to displacement of SST from 14°N to 2°N	Curve 2 of Fig. 2	15°N	33	Calculated by the model physics

(1971a) and off (1917b) the equator. Schneider (1977, 1983) found the nearly inviscid symmetric equilibrium atmospheric response to idealized ITCZ-like thermal forcing located at the equator (1977) and off the equator (1983). Held and Hou (1980) verified the nearly inviscid theory by numerical calculations and showed the effect of representing the thermal forcing as proportional to the incoming annual mean solar radiation. As the specified heat source of fixed intensity is moved away from the equator, the response should show the following features, so long as the assumptions that are made for the above calculations are valid:

1) Increased upper tropospheric tropical easterlies and

2) A meridional circulation response increasingly asymmetric about the equator. Two Hadley type cells, with rising branches coincident with the latitude of maximum ITCZ heating, should develop (rising occurs at this latitude so that the response is thermally direct and produces kinetic energy to balance dissipation). The Hadley cell which crosses the equator should become dominant in terms of meridional heat flux, and this cell should have an effective meridional extent that increases. The Hadley cell that is confined to the same hemisphere as the ITCZ should have decreasing meridional scale and heat flux. In the case of constant static stability, the Hadley cell mass fluxes and heat fluxes are proportional.

If the heat source is held fixed and the internal viscosity is reduced, the properties of the equilibrium response that are expected are 1) Increased jet stream zonal velocities, and a sharper meridional jet stream

structure, 2) Decreased meridional extent of the Hadley cells, and decreased vertically integrated meridional heat flux magnitudes, 3) The appearance of Ferrel cells flanking the Hadley cells at low enough internal viscosities and 4) No steady equilibrium solution for small enough internal viscosities.

1) RESPONSE TO PRESCRIBED HEAT SOURCES

Three heat sources were constructed for these experiments, a "spring" heat source (Fig. 3a) similar to that constructed by Newell *et al.* (1974) for March–May, a "summer" heat source (Fig. 4a) similar to Newell *et al.* for June–August, and a "monsoon" heat source (Fig. 5a) chosen somewhat arbitrarily by us. The dashed curves in the figures are the precipitation resulting from the vertical integral of the heat sources. The equilibrium response to the three heat sources was calculated. In experiment 1 with spring heating the spring SST distribution (curve 1 of Fig. 1) was used, while in experiments 2 (summer heating) and 3 (monsoon heating) the summer SST distribution (curve 2 of Fig. 1) was used. In these three experiments, the model was integrated to a steady state solution. Internal variability that appears in some of the integrations to be described below is due to the parameterizations of evaporation, moist convection, the interactive radiation water vapor calculation.

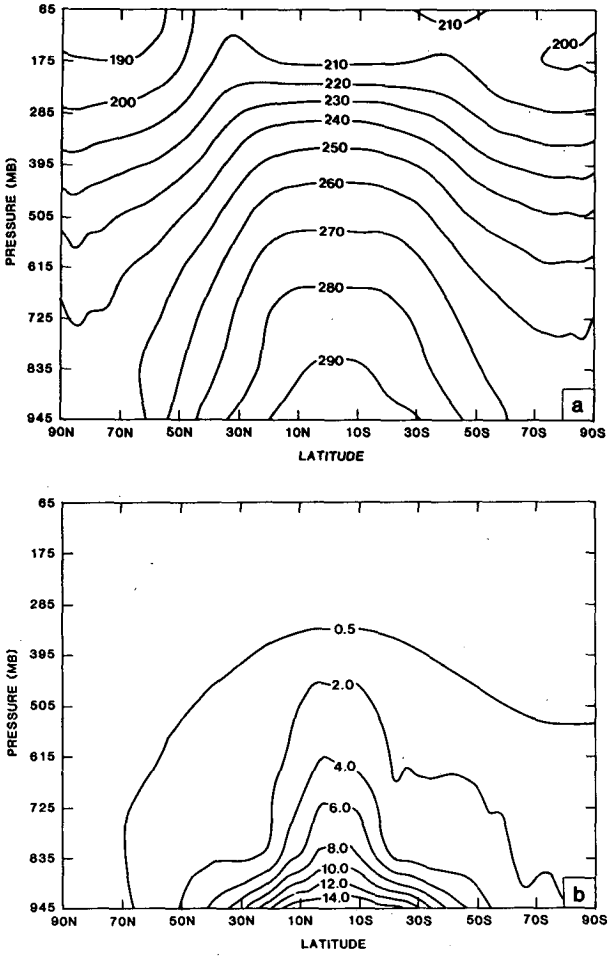

FIG. 2. Initial condition fields: (a) Temperature (K); (b) Specific humidity (g kg^{-1}). The other initial conditions are $U = V = 0$.

The results for the zonal winds, temperature, and stream functions in the steady state solutions of experiments 1, 2 and 3 are shown in Figs. 3, 4, and 5 respectively. The results qualitatively resemble the predictions of the simpler calculations, except that experiment 2 has weaker upper tropospheric tropical easterlies than with experiments 1 or 3. This seems to be due to the structure of the heating function chosen for experiment 1, which leads to air rising in the ITCZ above 505 mb originating from the ground near 10°S, a case not treated by Schneider (1977). In experiments 2 and 3 the ITCZ and the zero zonal wind line coincide. The strong equatorial upper tropospheric easterlies in the monsoon heating experiment are as expected. Also, the development of asymmetries in the heat fluxes, mass fluxes, and meridional extents of the Hadley cells are qualitatively as predicted by the earlier calculations. The differing vertical distributions of the spring and summer heat sources leads to different vertical distribution of tropical lapse rate in experiments 1 and 2 (as discussed by Schneider), so that heat and mass flux are not proportional to the intercomparison of the results of these experiments.

One significant feature of experiments 1 and 2 is the magnitude of the meridional mass flux, which is a factor of 2 (experiment 2) to 4 (experiment 1) times the observed (Oort and Rasmusson, 1971) Hadley cell mass fluxes in spring or summer. This feature apparently results from the neglect of cloud–radiative interaction in the radiative calculation. In terms of the Newtonian cooling approximation to radiation used by Schneider (1983), the radiative equilibrium lapse rate has been destabilized, at least in the upper troposphere, and the clear atmosphere radiative time constant is shorter than the time constant appropriate for the observed atmosphere. The removal of cloud-radiative feedback leads to a larger net outgoing longwave flux at the top of the atmosphere. The GLAS symmetric model without cloud-radiative feedback produces a net infrared radiative flux, averaged over the globe, of about 500 W m^{-2}, and about 400 W m^{-2} with cloud-radiative feedback included. These values are significantly larger than the solar radiation incident on the earth, approximately 340 W m^{-2}, the solar radiation absorbed by the earth's atmosphere and ocean, approximately 220 W m^{-2}. The effective model thermal driving is stronger than the thermal driving of the atmosphere. The effective radiative time constant of the model, using the formula of Giearasch *et al.* (1970), which is inversely proportional to the absorbed solar flux, is about half of the radiative time constant

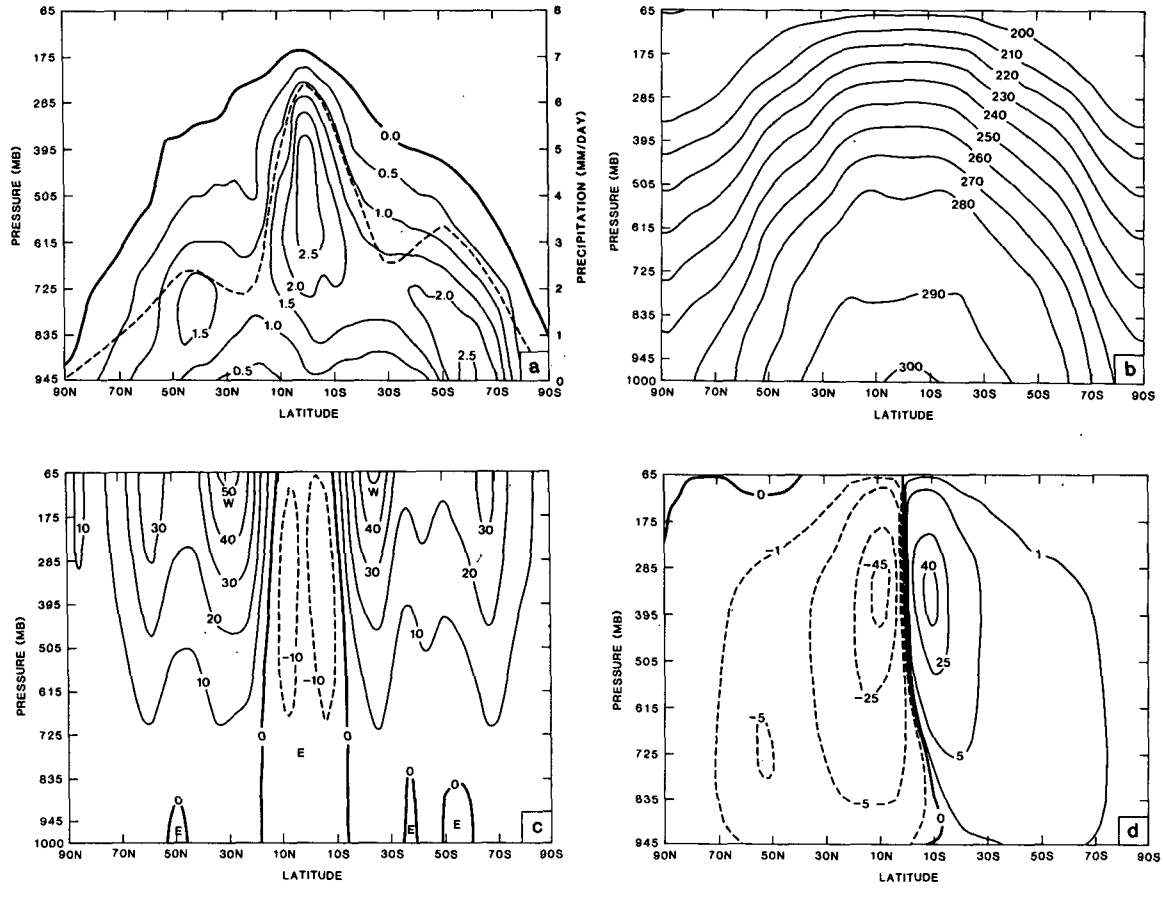

FIG. 3. Contours of solution to the symmetric circulation run—spring condition: (a) prescribed latent heating field, contours are K day^{-1}. The dashed curve represents equivalent precipitation distribution; (b) Temperature, contour interval 10 K; (c) zonal wind, contour interval 10 m s^{-1}; (d) streamfunction, contour 10^{10} kg s^{-1}.

of the atmosphere. According to the estimates of Schneider (1977) and Held and Hou (1980), the mass flux (or more correctly the heat flux) of the zonally symmetric Hadley circulation should be inversely proportional to the radiative time constant or directly proportional to the effective solar forcing. Thus the very large Hadley circulation mass fluxes produced by the GLAS symmetric model are ultimately a consequence of a prescribed SST distribution that is inconsistent with the actual solar forcing and calculated cloud cover. An internally consistent version of this symmetric model, which included a calculated oceanic heat budget, would have sea surface temperatures considerably lower than those which have been prescribed. The symmetric model run, with or without the cloud radiative feedback, produces time-averaged Hadley cell mass fluxes that are significantly stronger compared to the full climate model.

It can be seen by inspection of the lowest level streamfunction of experiments 1, 2 and 3 that the mass convergence at the top of the boundary layer is primarily induced by the latent heat source.

An additional spring run (experiment 4) with prescribed heating was carried out in which the vertically and horizontally integrated heating (and precipitation) was the same as shown in Fig. 2a, but the latitudinal structure was altered such that the heating rate was nearly uniform between 15°N and 15°S. The latent heating field, stream function, zonal wind and temperature for this run are shown in Fig. 5. It is seen that the strength of the Northern Hemisphere Hadley cell is considerably reduced with no appreciable change in the Southern Hemisphere Hadley cell. The strength of the upper level easterlies in the tropics is also reduced.

Another experiment (experiment 5) with summer SST distribution was also performed without any latent heat source. Using climatological water vapor for radiation leads to a near adiabatic lapse rate everywhere in the troposphere and a strong deep meridional circulation, with maximum mass flux 30×10^{10} kg s^{-1}. This experiment shows the role of deep cumulus heating in maintaining the stable tropical lapse rate. In this experiment the vertically integrated meridional

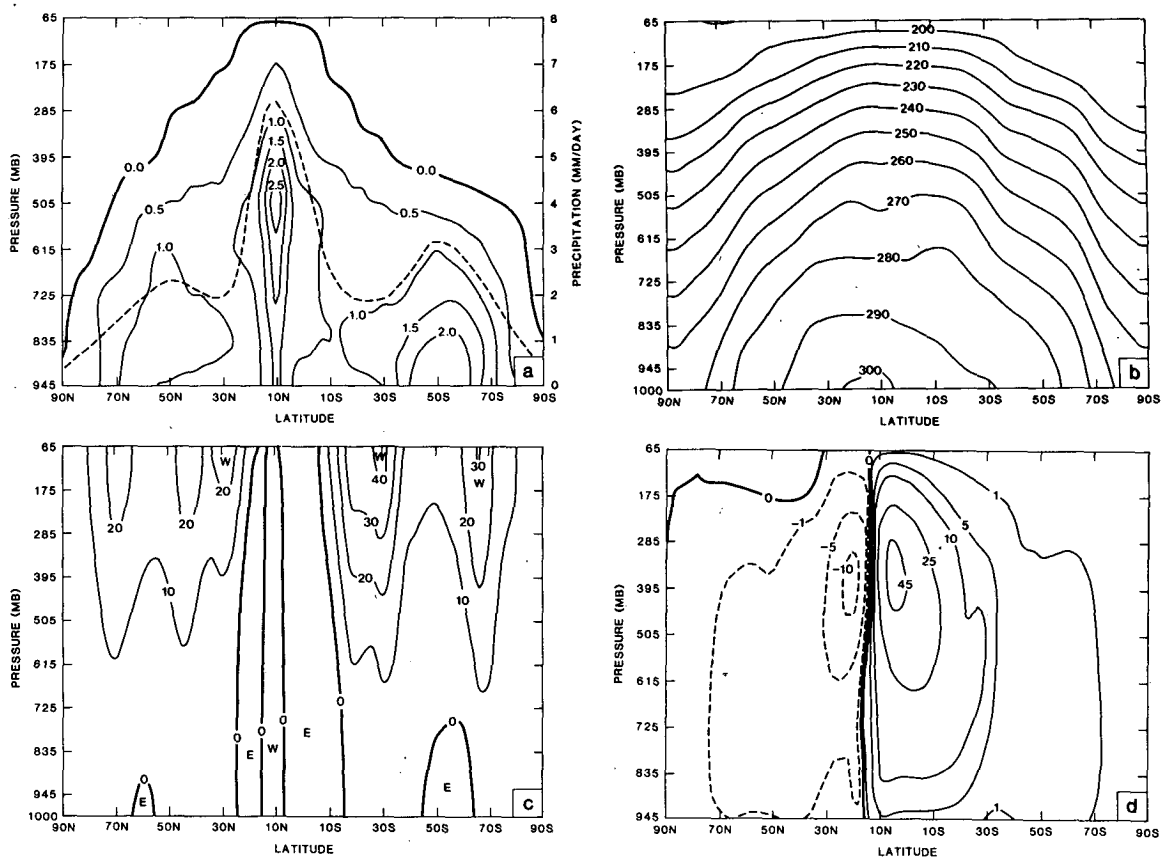

FIG. 4. As in Fig. 3 but for Northern Hemisphere summer condition.

heat flux is much reduced from that found in experiments 1–4, even though the Hadley mass flux is not much less.

2) RESPONSE TO PRESCRIBED INTERNAL VISCOSITY

In these experiments, the model was driven by the spring heating distribution and spring SSTs. The eddy viscosity as represented by the value at 505 mb, was taken $\nu_5 = 16.5$ m^2 s^{-1} (experiment 6) and $\nu_5 = 6.6$ m^2 s^{-1} (experiment 7). Steady state solutions were not obtained for smaller eddy viscosities. The streamfunction and zonal winds for experiments 6 and 7 are shown in Fig. 6. The corresponding results with $\nu_5 = 33$ m^3 s^{-1} are for experiment 1. As the eddy viscosity was reduced, some of the expected qualitative features were obtained; sharper and stronger jet streams, reduced Hadley cell meridional scales, and flanking Ferrel cells. Hadley cell heat fluxes were reduced in magnitude but the change in the Hadley cell extent led to tropical upper tropospheric lapse rates closer to adiabatic and a larger Hadley cell mass flux.

b. ITCZ experiments

The complete model including moisture budget, with moist convection and supersaturation sinks of water vapor and evaporative sources, was used to examine the behavior of the model produced ITCZ with various initial and SST boundary conditions (experiments 8–12). Internal viscosity was fixed, with value 33 m^2 s^{-1} at 505 mb. Some indication of the relative effects of SST and CISK processes is gained from these calculations. In each of the cases considered, a statistical equilibrium ITCZ eventually developed over the SST maximum; however, the CISK process is effective in producing an ITCZ of the narrowest possible meridional scale and in producing persistence of non-equilibrium ITCZs.

1) RESTING UNBALANCED ATMOSPHERE INITIAL CONDITIONS

Two experiments were performed with initial conditions consisting of a resting atmosphere, and the temperature and water vapor mixing ratio distributions shown in Fig. 2. In experiment 8, the spring SST distribution (curve 1 of Fig. 1) was imposed as a lower boundary condition, while in experiment 9, the Northern Hemisphere summer SST distribution (curve 2 of Fig. 1) was used as a lower boundary condition. The initial conditions for the winds and temperatures in these experiments were highly unbalanced, since there

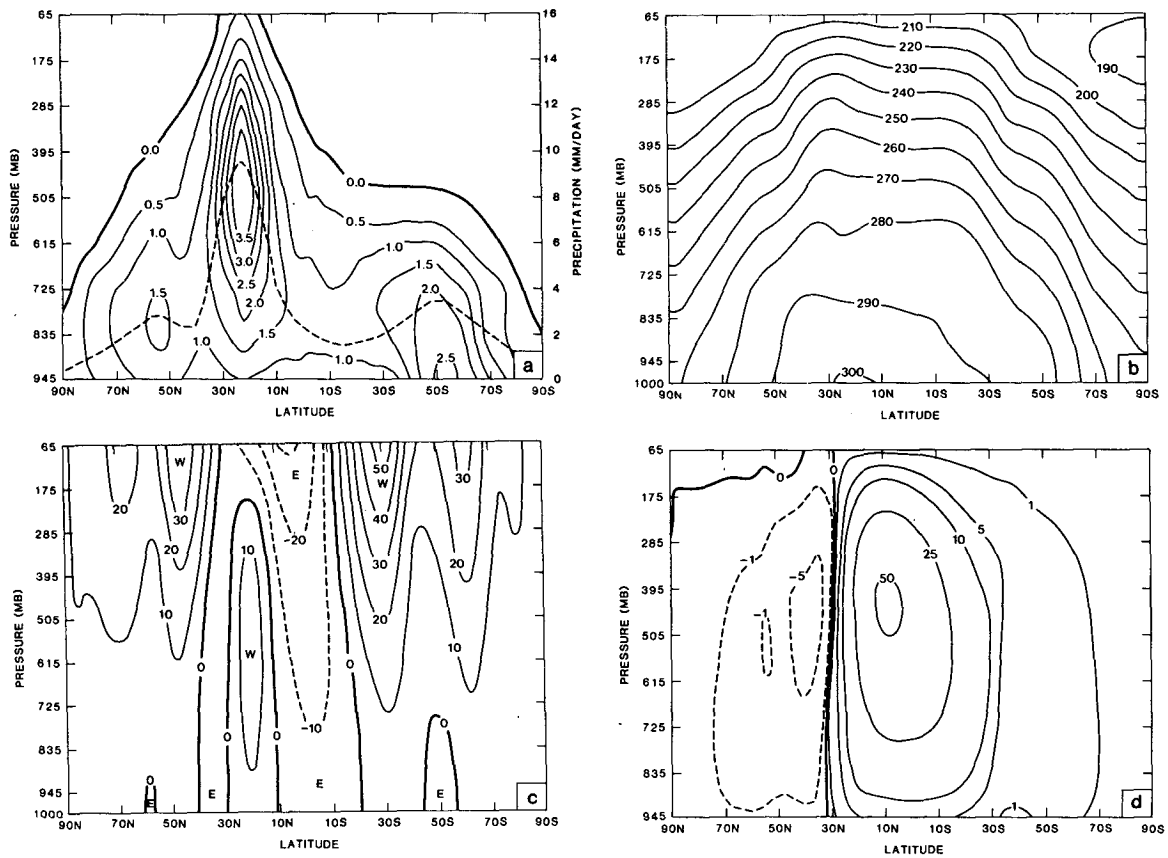

FIG. 5. As in Fig. 3 but for south Asian monsoon condition.

is no Coriolis force to compensate the horizontal pressure gradients implied by the temperature distribution. Therefore, the initial stages of the calculations are dominated by strong meridional acceleration which produce meridional motions that adjust the atmosphere toward a balanced or geostrophic state by redistributing angular momentum and heat. After about a two month adjustment, statistical equilibrium solutions were obtained with the ITCZ at a fixed position.

The time mean solutions averaged over days 91–150 are shown for experiment 8 (Fig. 8) and experiment 9 (Fig. 9). In experiment 8 the equilibrium ITCZ occurs at 2°S, while in experiment 9 the ITCZ occurs at 14°N. These are the latitudes of maximum SST in each case. The ITCZs that develop are very narrow; the convective heating and rising branches of the Hadley cells occur at a single latitudinal grid point. This structure corresponds to the most rapidly growing CISK solutions (Charney, 1971). CISK is apparently responsible for the meridional structure of the ITCZ, while the location is determined by the SST distribution in this model, as also found in the symmetric model of Schneider (1977). The latent heating field for experiment 9, with Northern Hemisphere summer SST is shown in Fig. 10. The latent heating is due almost entirely to moist convection located at 14°N and reaching magnitudes of more than 10 K day^{-1} between 725 and 395 mb. The structure of the apparent convective latent heating is that of a heat source which is almost disconnected from the boundary layer. Apparently, however, there is a large enough proportion of the latent heating near the top of the boundary layer for CISK to operate.

The meridional circulations for experiments 8 and 9 (Figs. 8c and 9c) have the asymmetrical structure and variation of intensity predicted by the theoretical calculations mentioned in Section 3. Again, the Hadley cell mass fluxes are quite large, a factor of more than 3 times larger than those expected from observations. Additionally, a very large proportion, 80–90% of the total mass flux, is made up of air which never enters the boundary layer and which consequently is dry and moist convectively stable. As upward velocity and latent heating must be highly correlated in the tropical ITCZ for dynamical reasons, this feature of the results must be due to combined effects of intrinsic properties of the moist convection parameterization and radiative calculations. It is clear from the most basic consideration and observations (Riehl and Malkus, 1958) that in essence all rising motion above the tropical boundary layer occurs in association with condensation, hence in clouds and primarily in cumulus type clouds. The distribution of upward mass flux in the

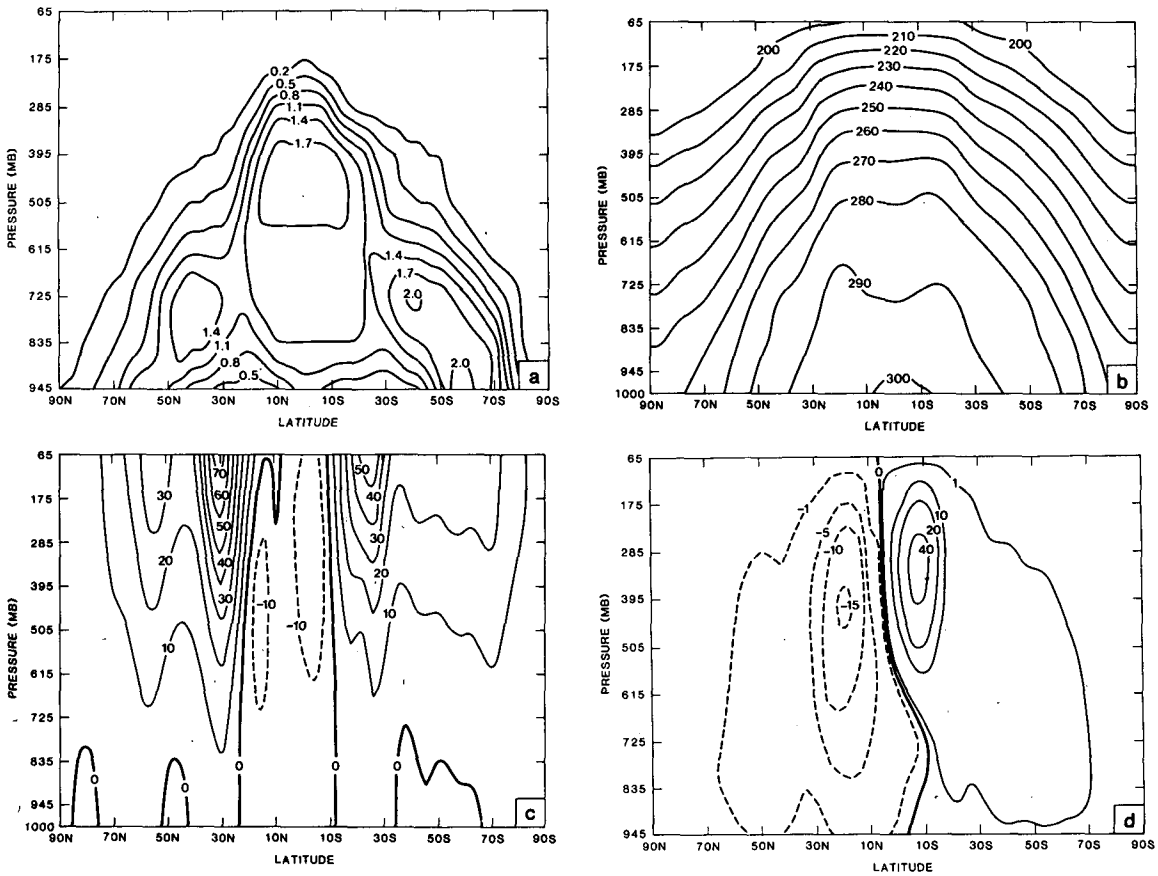

FIG. 6. Response of the Hadley circulation to a broad tropical heat source. The coefficient of the vertical eddy viscosity at the middle layer for this run is 16.5 $m^2 s^{-1}$: (a) prescribed latent heating (K day^{-1}), (b) temperature (K), (c) zonal winds (m s^{-1}), (d) streamfunction (10^{10} kg s^{-1}).

ITCZ, particularly in these calculations where radiation is a negligible component of the ITCZ heat budget, is the model's representation of the mass flux in deep cumulus clouds. Cumulus mass flux can increase above cloud base only by entrainment of the surrounding dry, stable air. It is unlikely that in reality a cloud could entrain the amount of dry air implied by these results.

2) RESPONSE OF EQUILIBRIUM ITCZ TO SST PROFILE

In these experiments, (10–12) an equilibrium ITCZ solution was generated as in experiments 8 and 9 at the SST maximum. Then the integration was continued using a different specified SST with a maximum at a different latitude. Eventually the equilibrium ITCZ developed at the new SST maximum. The transient behavior involved in the adjustment of persistence and then a discontinuous jump in ITCZ position was interesting and is described as follows.

In experiment 10, the 14°N ITCZ equilibrium solution, generated in experiment 9 using summer SST (curve 2 of Fig. 1), was taken for the initial conditions and the spring SST (curve 1 of Fig. 1) was used as the lower boundary condition. The vertical velocity at 505 mb (not shown) as a function of latitude and time for this calculation showed that the ITCZ persisted at 14°N for about 3 months with moist convection suppressed elsewhere. Then a double ITCZ formed at 14°N and 2°N, and this structure was maintained for a period of about 10 days. During these ten days the ITCZ at 14°N was steadily weakening and at 2°N it was strengthening. Finally, the 14°N ITCZ disappeared, and the equilibrium solution with ITCZ at 2°N was obtained. Apparently, the initial 14°N ITCZ maintains itself in place by a CISK-like process and suppresses convection elsewhere in the tropics by the large scale response (sinking which leads to subtropical deserts on Earth). However, the SST gradient induced boundary layer moisture convergence eventually led to moist convection at the SST maximum, which leads to the growth of a new ITCZ and associated large scale response at this latitude. The new ITCZ reduced the moisture supply to the other ITCZ, and eventually suppressed it altogether. The ITCZ never occurred at latitudes between its initial and final positions. Presumably then, if SST were to change continuously,

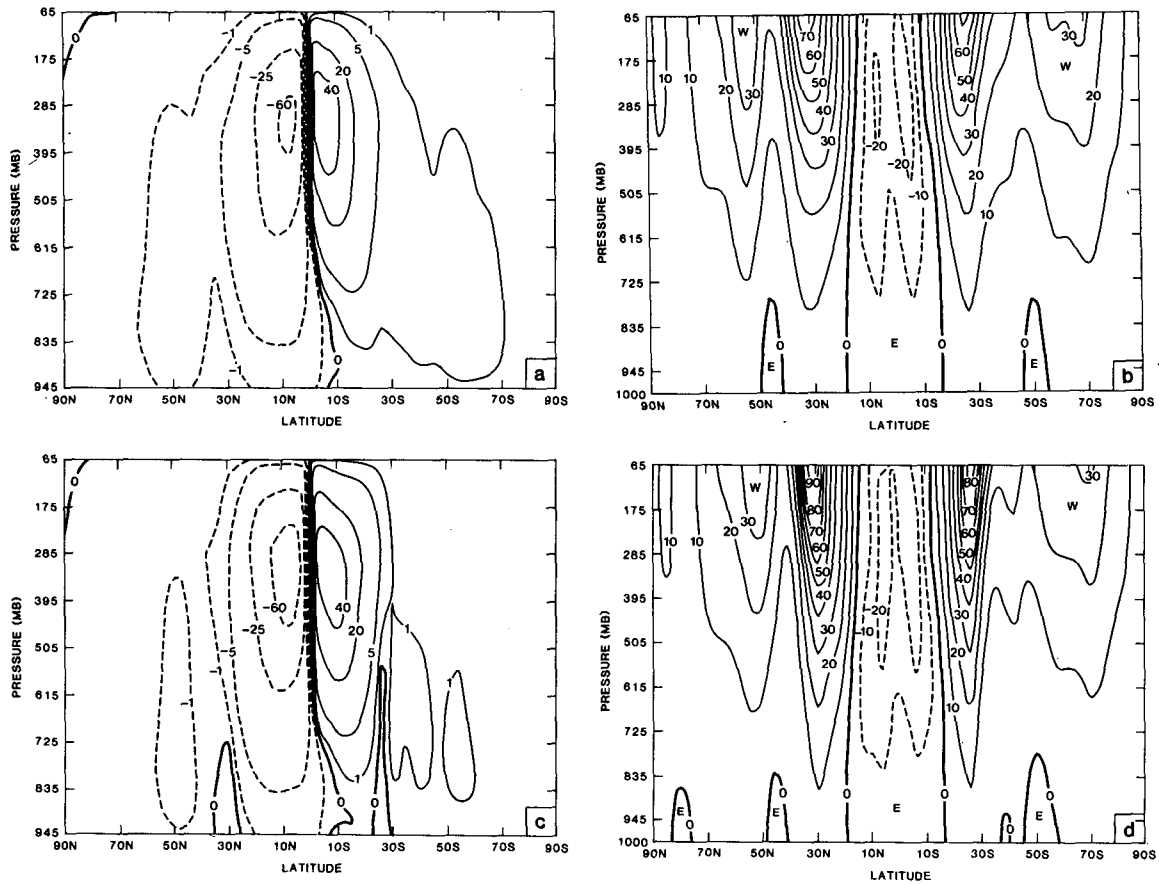

FIG. 7. Streamfunction and zonal winds for two runs with reduced vertical eddy viscosity: (a)–(b) streamfunction and zonal winds corresponding to the run with $\nu_5 = 16.5$ m^2 s^{-1}; (c)–(d) streamfunction and zonal winds corresponding to the run with $\nu_5 = 6.6$ m^2 s^{-1}. Units are the same as in Fig. 3.

the ITCZ would follow the SST maximum if the SST changes were slow enough and it would move by jumps if the SST changes were rapid.

In order to investigate the effect of the magnitude of the SST changes on the time scale for the ITCZ adjustment process, experiment 11 was performed. The initial conditions were the same as for experiment 10, but the SST distribution with its maximum at 2° was obtained by shifting the summer SST curve in latitude. This produced an SST 1.5 K warmer at 2° than at 14° in contrast to the SST difference of 0.5 K used in experiment 10. The same qualitative features as in experiment 10 were found. The vertical velocity at 500 mb as a function of latitude and time is shown in Fig. 11. It is seen that a persistent ITCZ occurs at 14°N, then double ITCZs at 2°N and 14°N followed by an equilibrium ITCZ at 2°N. However, the persistent 14° ITCZ lasted only for 3 weeks, as opposed to a period of 3 months in experiment 10. The duration of the persistence of the initial ITCZ was approximately proportional to the 2–14°N SST difference.

The last experiment examined the effect of reversing the procedure of experiment 11. The equilibrium solution of experiment 11 (2°N ITCZ) was used as initial condition, and the SST taken as the original summer SST with maximum at 14°N. The transient behavior of this calculation was somewhat different from that of experiments 10 and 11. The 505 mb latitude–time vertical velocity for experiment 12 is shown in Fig. 12. In this case, the ITCZ did not persist for very long at its initial position, 2°N. Within 10 days following the start of the experiment, the 2°N ITCZ disappeared, and a new ITCZ formed at 22°N. Then, the ITCZ persisted in this position for about 60 days. Finally, it moved to 14°N, the latitude of the SST maximum. This behavior seems to be due to evaporation-induced CISK. Shifting the SST curve leads to SST changes that become larger at higher latitudes. At 22°N the new SST is several degrees warmer compared to the surface air. This configuration produced strong evaporation, conditional instability, and a configuration favorable for CISK to operate. SST gradients are best able to produce boundary layer mass convergence near the equator (Schneider and Lindzen, 1976). We are unable to explain why the ITCZ initially formed at 22°N rather than at some other latitude, but suggest

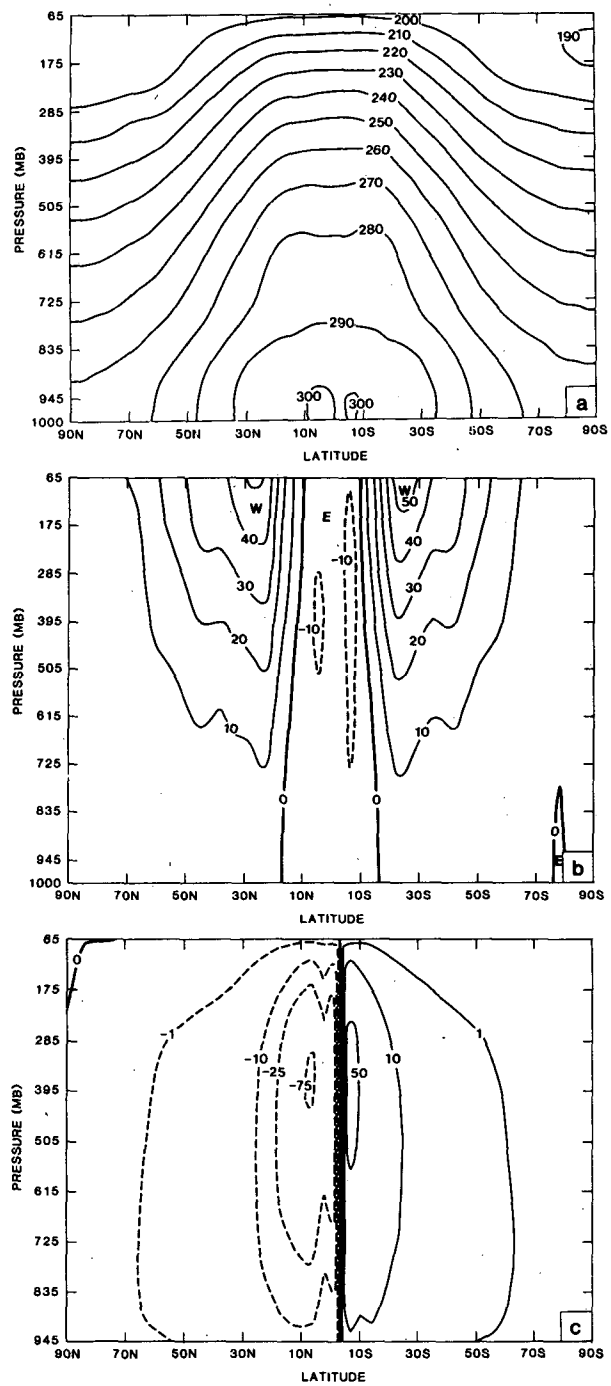

FIG. 8. Contours of solution to the global ocean run with hydrology—spring conditions: (a) temperature, contour interval 10 K; (b) zonal wind, contour interval 10 m s^{-1}; (c) streamfunction, contour 10^{10} kg s^{-1}.

that this may have to do with the competition between the induced evaporation and distribution of the boundary layer mass divergence of the initial conditions. We are also unable to explain the quick disappearance of the 2°N ITCZ as the SST changes at this latitude are the same as those of experiment 11 at the initial ITCZ positions and the ITCZ was initially persistent in that case.

4. Conclusions and discussion

A zonally symmetric version of the GLAS Climate Model has been constructed, and the results of some initial integrations have been discussed. The Model

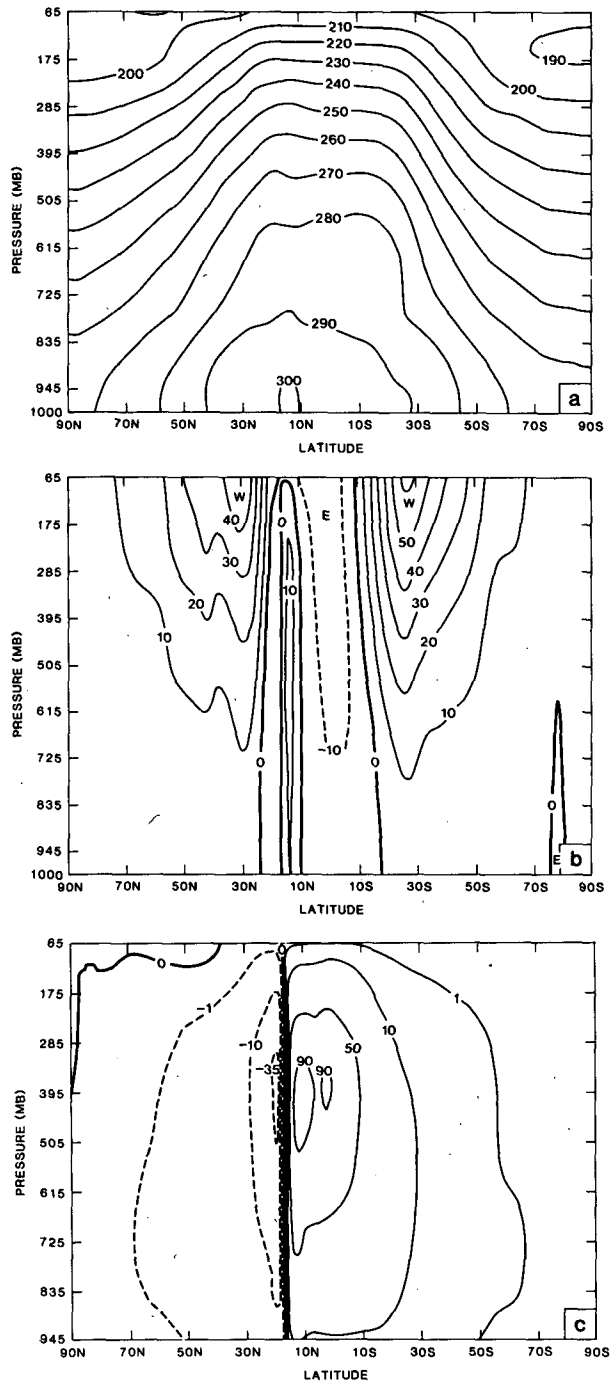

FIG. 9. As in Fig. 8 but for Northern Hemisphere summer condition.

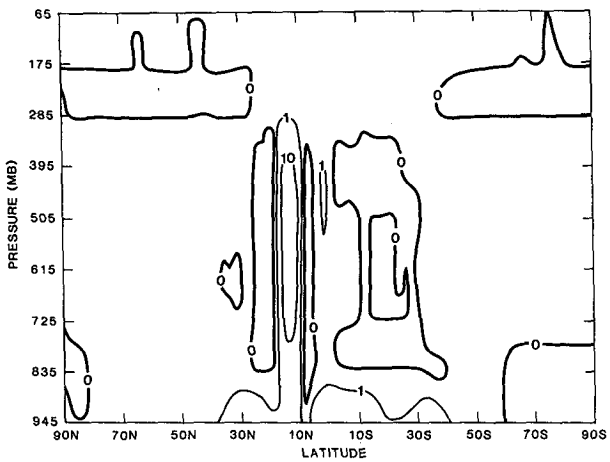

FIG. 10. The latent heating field (K day^{-1}) for the all ocean run—Northern Hemisphere summer condition.

should be useful for understanding and predicting the behavior of the complete GCM and as a research tool to generate questions and to examine theoretical predictions. As far as evaluation of the GCM performance, the fixed heat source and ITCZ experiments indicate that the model representation of zonally symmetric dynamics is adequate, as the prediction of simplified theories are qualitatively reproduced. Insofar as the model parameterization of physical processes is concerned, the symmetric model calculations leads to the following conclusions: 1) The cloud–radiative feedback parameterization is responsible for a significant amount of the model's internal variability in the tropics. When SST distributions are prescribed, the model should be modified to obtain a correct representation of the balance between incoming and outgoing radiation. 2) The moist convective parameterization plays an important role in determining the intensity of the Hadley circulation and moist convective parameterization.

Thus the symmetric model results suggest that improvement of the GCM physics can be obtained through 1) incorporation of a moist convection parameterization based on prediction of the vertical distribution of cumulus mass flux rather than convective adjustment and 2) an approach to cloud–radiative feedback and SST prediction that automatically leads to the correct representation of the globally integrated heat budget. This requires the modeling of the oceanic as well as the atmosphere and land surface heat budget.

The model, including the prediction of the moisture field, was used for some experiments designed to examine the processes controlling the position of the zonally symmetric ITCZ. For a wide variety of initial conditions, it was found that, eventually, a narrow equilibrium ITCZ always formed over the SST maximum. When the initial conditions were chosen to be a model produced equilibrium, consistent with some SST distributions, and a different SST distribution was taken as lower boundary condition, the ITCZ was initially persistent in the case where the ultimate equilibrium ITCZ was equatorwards of its initial position. This result seems to indicate that CISK and SST processes are competitive, although, at least for the small number of cases considered, the SST effect eventually won out. In the case where the final ITCZ position was polewards of its initial position, the initial ITCZ did not persist, but passed through an intermediate persistent stage where it existed polewards of its final position. Changes in ITCZ position appeared to occur

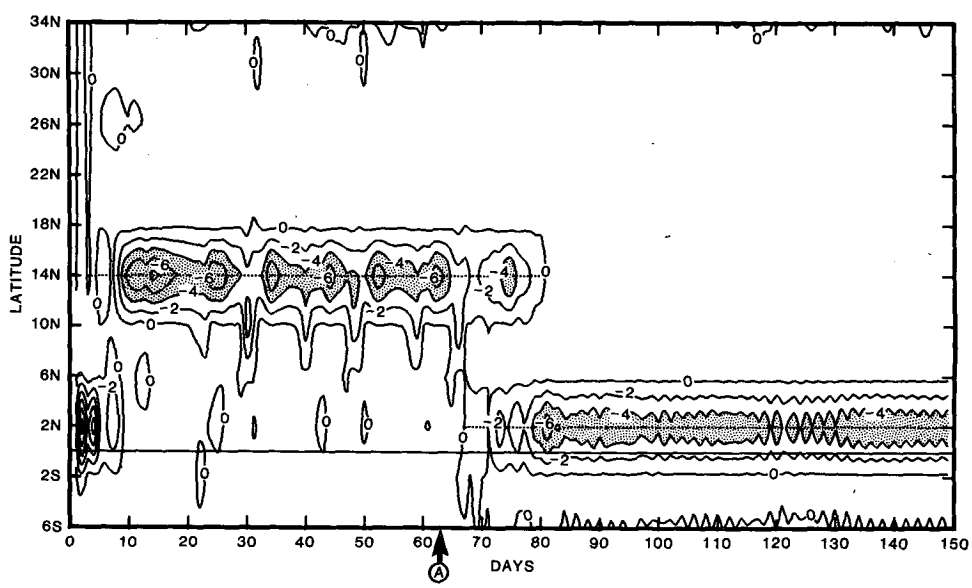

FIG. 11. Vertical velocity (ω) in 10^{-5} mb s^{-1} averaged between levels 3 and 7. On day 64 (shown at A) SST profile was shifted southwards from maxima at 14°N to 2°N.

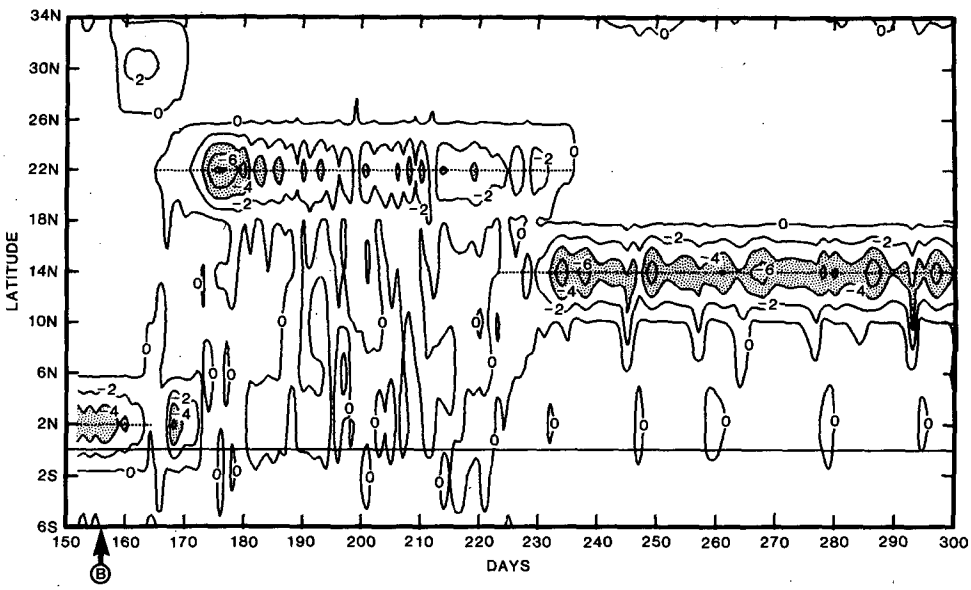

FIG. 12. Vertical velocity (ω) in 10^{-5} mbs^{-1} averaged between levels 3 and 7. On day 156 (shown at B) SST profile was shifted from maxima at 2°N to 14°N.

by jumps, rather than by continuous displacements. Studying this interesting phenomenon may be the object of future research.

In this paper we have examined only the time averaged circulation. We have also examined the time series of the simulated fields. It was found that for the simulations in which heating was determined by the model physics, the strength of the Hadley cell showed episodes of strong and weak intensity. This quasi-periodic behavior of the Hadley cell has been analysed in an accompanying paper (Goswami and Shukla, 1984).

Problems currently under investigation with the GLAS symmetric model include an attempt to produce multiple CISK induced equilibria when the SST and solar forcing are specified to be independent of latitude, and the study of the dynamics of an internally consistent zonally symmetric coupled ocean-atmosphere or ocean-atmosphere-land climate model.

Acknowledgments. The studies with the symmetric GCM were initiated by the late Prof. J. G. Charney and we benefited greatly from discussions with him.

We are grateful to Drs. E. Kalnay and D. Randall for many discussions. We are especially thankful to Mr. L. Marx for his help in producing the symmetric version of the GLAS Climate Model. The authors are pleased to acknowledge the help provided by Miss Lena Fornito in processing the results, Laura Rumburg for drafting the figures and Mary Ann Wells for her help in typing the manuscript. The work of one of the authors (BNG) was supported in parts by National Research Council, Washington, D.C. and Universities Space Research Association, Columbia, Md.

REFERENCES

Arakawa, A., 1972: Design of the UCLA General Circulation Model. *Numerical Simulation of Weather and Climate,* Tech. Rep. No. 7, Dept. Meteor., UCLA.

——, and V. R. Lamb, 1977: Computational design of the basic dynamical processes of the UCLA general circulation model. *Methods in Computational Physics,* Vol. 17, Academic Press, 265 pp.

Charney, J. G., 1968: The Intertropical Convergence Zone and the Hadley circulation of the atmosphere. Unpublished manuscript.

——, 1969: The Intertropical Convergence Zone and Hadley Circulation of the Atmosphere. *Proc. of WMO/IUGG Symp. NWP,* Tokyo, Meteor. Soc. Japan, III-73.

——, 1971: Tropical cyclogenesis and the formation of the Intertropical Convergence Zone. *Mathematical Problems of Geophysical Fluid Dynamics,* W. H. Reid, Ed., *Lectures in Applied Mathematics,* Vol. 13, Amer. Math. Soc., 355–368.

——, 1973: Planetary Fluid dynamics, Chapter III. Symmetric circulation in idealized models. *Dynamic Meteorology:* Lecture Delivered at the Summer School of Space Physics of the Centre National d'etudes Spatiales, Lammion, France, P. Morel, Ed., D. Reidel, 128–141.

Dickinson, R. E., 1971a: Details of the model and simulation of gross features of zonally mean troposphere. *Mon. Wea. Rev.,* **99,** 501–510.

——, 1971b: Variation of tropospheric mean structure with season and differences between hemispheres. *Mon. Wea. Rev.,* **99,** 511–523.

Estoque, M. A., and M. Douglas, 1978: Structure of the intertropical convergence zone over GATE area. *Tellus,* **30,** 55–61.

Giearasch, P., R. M. Goody and P. Stone, 1970: The energy balance of planetary atmospheres. *Geophys. Fluid Dyn.,* **1,** 1–8.

Godson, W. L., 1955: The computation of infrared transmission by atmospheric water vapor. *J. Meteor.,* **12,** 272–284.

Goswami, B. N., and J. Shukla, 1984: Quasi-periodic oscillations in a symmetric general circulation model. *J. Atmos. Sci.,* **41,** 20–37.

Gruber, A., 1972: Fluctuations in the position of the ITCZ in the Atlantic and Pacific Oceans. *J. Atmos. Sci.,* **29,** 193–197.

Held, I. M., and A. Hou, 1980: Nonlinear axially symmetric circulations in a nearly inviscid atmosphere. *J. Atmos. Sci.*, **37**, 515–533.

Hubert, L. J., A. F. Krueger and J. S. Winston, 1969: The double Intertropical Convergence Zone—Fact or fiction? *J. Atmos. Sci.*, **26**, 771–773.

Hunt, B. G., 1973: Zonally symmetric global general circulation models with and without hydrologic cycle. *Tellus*, **25**, 337–354.

Kornfield, J., A. F. Hasler, K. J. Hanson and V. E. Suomi, 1967: Photographic cloud climatology from ESSA III and V computer produced mosaics. *Bull. Amer. Meteor. Soc.*, **48**, 878–883.

Lacis, A. A., and J. E. Hanse, 1974: A parameterization for the absorption of solar radiation in the earth's atmosphere. *J. Atmos. Sci.*, **31**, 118–133.

Lorenz, E. N., 1960: Energy and numerical weather prediction. *Tellus*, **12**, 364–373.

——, 1967: *Nature and Theory of the General Circulation of the Atmosphere.*, WMO No. 218., World Meteorological Organization, 115 pp.

Miller, D. B., and R. G. Feddes, 1971: *Global Atlas of Relative Cloud Cover, 1967–1970, Based on Photographic Signals from Meteorological Satellites.* U.S. Dept. of Commerce and U.S. Air Force, 237 pp. [NTIS No. AD739434].

Newell, G. R., J. W. Kidson, D. G. Vincent and G. J. Boer, 1974: *The General Circulation of the Tropical Atmosphere*, Vol. 2. The MIT Press.

Oort, A. H., and E. M. Rasmusson, 1970: On the annual variation of the monthly mean meridional circulation. *Mon. Wea. Rev.*, **98**, 423–422.

——, and ——, 1971: *Atmospheric Circulation Statistics.* U.S. Department of Commerce, NOAA Prof. Pap. No. 5, 434 pp. [NTIS No. AD F 39].

Pike, A. C., 1971: Intertropical Convergence Zone studied with an interacting atmosphere and ocean model. *Mon. Wea. Rev.*, **99**, 469–477.

Riehl, H., 1979: *Climate and Weather in the Tropics.* Academic Press, 661 pp.

——, and J. S. Malkus, 1958: On the heat balance of the equatorial trough zone. *Geophysica*, **6**, 503–538.

Sadler, J. C., 1975: The monsoon circulation and cloudiness over the GATE area. *Mon. Wea. Rev.*, **103**, 369–387.

Saha, K., 1971: Mean cloud distributions over tropical ocean. *Tellus*, **23**, 183–194.

Schneider, E. K., 1977: Axially symmetric steady state models of the basic state for instability and climatic studies. Part II: Nonlinear calculations. *J. Atmos. Sci.*, **34**, 280–296.

——, 1983: Martian great dust storm: Interpretive axially symmetric models. *Icarus*, (in press).

——, and R. S. Lindzen, 1976: The influence of stable stratification on the thermally driven tropical boundary layer. *J. Atmos. Sci.*, **33**, 1301–1307.

——, and ——, 1977: Axially symmetric steady state models of the basic state of instability and climate studies. Part I: Linearized calculations. *J. Atmos. Sci.*, **34**, 23–279.

Shukla, J., D. Straus, D. Randall, Y. Sud and L. Marx, 1981: Winter and summer simulations with the GLAS Climate Model. NASA Tech. Memo. 83866, 282 pp. [NTIS No. N8218807].

Somerville, R. C. J., P. H. Stone, M. Halem, J. E. Hansen, H. S. Hogan, L. M. Druyan, G. Russell, A. A. Lacis, W. L. Quirk and J. Tenenbaum, 1974: The GISS model of the global atmosphere. *J. Atmos. Sci.*, **31**, 84–117.

Sud, Y. C., and J. A. Abeles, 1981: Calculation of surface temperature and surface fluxes in the GLAS GCM. NASA Tech. Memo. 82167, 13 pp. [NTIS No. N8129697].

——, and M. J. Fenessy, 1982: An observational data based evapotranspiration function for general circulation models. *Atmos.–Ocean*, **20**, 301–316.

World Meteorological Organization, 1978: *The West African Monsoon Experiment (WAMEX)*, GARP Publ. Ser. No. 21, ICSU/WMO.

Wu, M. L., 1980: The exchange of infrared radiative energy in the troposphere. *J. Geophys. Res.*, **85**, 4084–4090.